RESEARCH ARTICLE

Macromolecular Reaction Engineering
www.mre-journal.de

Surface Molecularly Imprinted Cellulose-Synthetic Hybrid Particles Prepared via ATRP for Enrichment of Flavonoids in Olive Leaf

Catarina P. Gomes, Rolando C. S. Dias, and Mário Rui P. F. N. Costa*

Surface molecularly imprinted cellulose-synthetic hybrid particles are prepared via atom transfer radical polymerization (ATRP). The two-step process involves the immobilization of α-bromoisobutyryl bromide in the pristine microcrystalline cellulose, to generate ATRP macroinitiator particles, and then the creation of a crosslinked-imprinted shell in the particles surface considering ATRP of 4-vinylpyridine (4VP) and ethylene glycoldimethacrylate (EGDMA) with quercetin as imprinting template. Among the polymerization recipes tested, a system with ethanol as solvent preserves a final size of the hybrid particles suitable for application as adsorbent, while also incorporating the 4VP/EGDMA co-monomers. Testing of imprinted/non-imprinted particles for sorption/desorption of standard phenolic compounds shows the modification of the surface of the pristine cellulose and also the achievement of molecular imprinting (imprinting factor ≈2.6). Particles are used for the enrichment of flavonoids in olive leaf extracts and the special features of the developed molecularly imprinted adsorbents are again highlighted with this complex mixture of phenolic compounds. It is shown that production of fractions rich in luteolin-7-O-glucoside, apigenin-7-O-glucoside, or quercetin, among other flavonoids is possible (estimated enrichment factors up to 4). These results point up for the usefulness of natural-synthetic materials with processes to get high-added value compounds in the framework of circular bio-economy.

1. Introduction

Cyclic sorption/desorption processes are widely used in industry as well as in analytical procedures to make separation and purification of target compounds. Adsorbents for these applications range from natural materials and their modified counterparts (e.g., activated carbons, silica-based, other minerals, lignocellulosic/polysaccharides) to synthetic polymer resins (e.g., the industrially relevant Amberlite, Supellite, or Reillex resins). Durability, stability, ease of regeneration, and the possibility to create tailored active materials are important benefits associated with synthetic polymer resins. Environmental protection, biotechnology, pharmaceutics and chemicals production are application fields with a large-scale use of polymer resins for separation and purification.

Nowadays, a growing effort is being observed for the valorization of agricultural residues and sub-products, namely, through the enrichment and isolation of compounds with high-added value. This downstream processing approach is being considered with many systems in the framework of sustainability and circular bio-economy policies. A specific case with high potential economic relevance concerns the valorization of olive leaf. Indeed, around 4.5 million tons of leaves are generated each year as a by-product of the olive and olive-oil production. These olive leaves must be removed from the fields and olive-mills. Usually they are either burned, or simply used as fuels or for animal feed. However, olive leaf is extremely rich in bio-resources, being estimated to contain around 1 million tons of bioactive compounds, 1 million tons of cellulose, and 1.5 million tons of lignin which are currently underexploited.[1] In particular, the extraction and isolation of high-added value bioactive compounds in olive leaf (e.g., different kinds of polyphenols and triterpenoids) is especially appealing due to their high-market potential in the food, feed, chemical, nutraceutical, cosmetic, and pharmaceutical sectors.[1]

Extraction, followed by sorption/desorption processes (to purify and concentrate liquid mixtures), is often considered to get target compounds from plant residues and sub-products. Actually, a key issue in this field concerns the processing of diluted streams with the presence of many unwanted compounds.

C. P. Gomes, R. C. S. Dias
Centro de Investigação de Montanha (CIMO), Instituto Politécnico de Bragança
Campus de Santa
Bragança 5300 253, Portugal
E-mail: rdias@ipb.pt
M. R. P. F. N. Costa
LSRE, Faculdade de Engenharia da Universidade do Porto
Rua Roberto Frias s/n
Porto 4200-465, Portugal

The ORCID identification number(s) for the author(s) of this article can be found under https://doi.org/10.1002/mren.202300011

DOI: 10.1002/mren.202300011

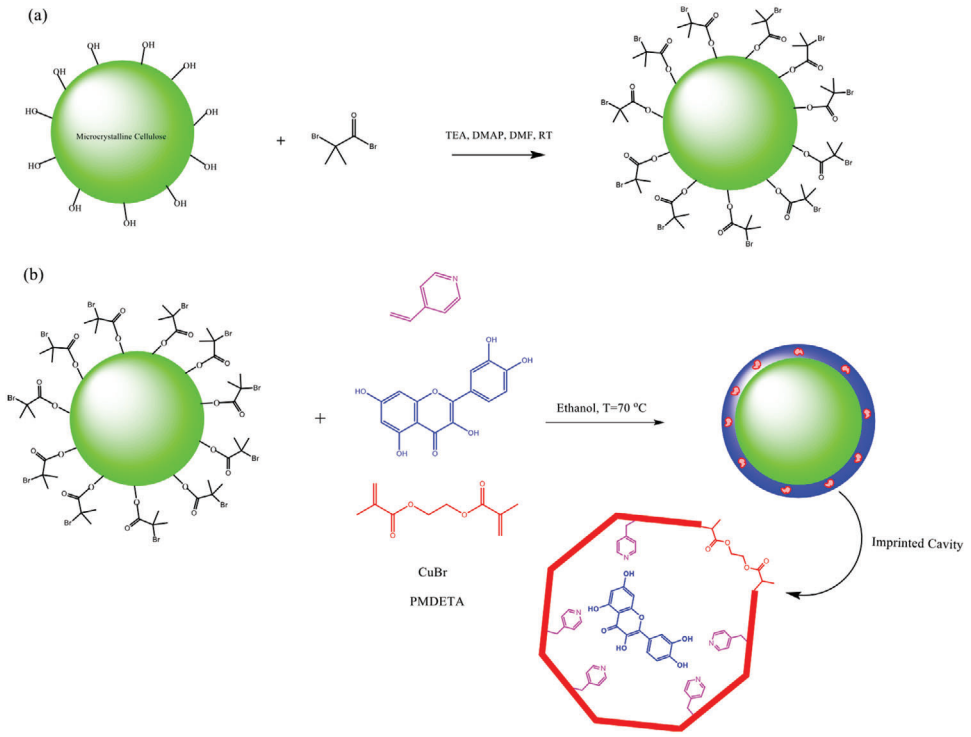

Figure 1. Depiction of the synthesis procedure considered for the development of surface molecularly imprinted cellulose-synthetic hybrid particles via ATRP. a) Immobilization of α-bromoisobutyryl bromide in pristine microcrystalline cellulose (MCC) to generate ATRP macroinitiator particles (MCC-Br). b) Grafting of a crosslinked-imprinted shell in the particles surface considering ATRP of co-monomers 4VP/EGDMA in the presence of quercetin.

Solvent evaporation (with possible thermal effects on bioactive compounds) and/or crystallization (difficult with complex mixtures) are energetically demanding and challenging in view of the use of sustainable, efficient, and economically feasible industrial applications. Harsh conditions requiring considerable cost and energy expenditure are in general inherent to crystallization for separation, purification, and downstream production (technology based on solvent evaporative methods). Therefore, the lower energy consumption, cyclability, preservation of temperature-sensitive compounds, operational flexibility, amenability to intensification, and industrial scalability make sorption/desorption processes attractive in this domain. Nowadays, membrane-supported selective separation is also playing an important role in this field. In practice, the valorization of underutilized effluents derived from olives debittering, artichoke washing, olive oil or natural juices production, among many others, is being already made with sorption/desorption processes.[2]

Here, we address the development of tailored adsorbents and their application in sorption/desorption processes for the enrichment of flavonoids in olive leaf extracts. Surface molecularly imprinted cellulose-synthetic hybrid particles, prepared via atom transfer radical polymerization (ATRP), were developed to assess the combination in the same material of high retention capability (selection of appropriated synthetic functional monomers), selectivity toward target compounds (molecular imprinting), enhancement of binding site accessibility, and high mass transfer (particles with active surface). These features are joined in core–shell particles with cellulose core, highlighting the possibility for generation of advanced natural-synthetic materials with application in the development of sustainable processes in the framework of circular bio-economy.

The synthesis approach here considered for surface molecular imprinting (see a recent overview on the subject in ref. [3]) includes: i) the immobilization of α-bromoisobutyryl bromide in pristine microcrystalline cellulose (MCC) to generate ATRP macroinitiator particles (MCC-Br) and ii) the grafting of a crosslinked-imprinted shell in the surface of these particles through ATRP with 4-vinylpyridine (4VP) as functional monomer, ethylene glycol dimethacrylate (EGDMA) as crosslinker, and quercetin as the flavonoid template. Selected imprinted particles are assessed with standard polyphenol compounds and also with an industrial olive leaf extract. The production of flavonoid-enriched fractions from the complex olive leaf extract, through sorption/desorption processes with developed imprinted particles, is highlighted.

2. Results and Discussion

2.1. Rationale for Materials Synthesis

The reaction steps here considered for the synthesis of surface molecularly imprinted cellulose-synthetic hybrid particles are depicted in **Figure 1**. Our approach follows the previous related works with ATRP surface grafting in cellulose.[4–6] The first step (Figure 1a) concerns the immobilization of α-bromoisobutyryl bromide (BIBB) in MCC through the reaction with OH groups. Confirmation for the generation of the ATRP macroinitiator MCC-Br was performed using Fourier transform infrared (FTIR),

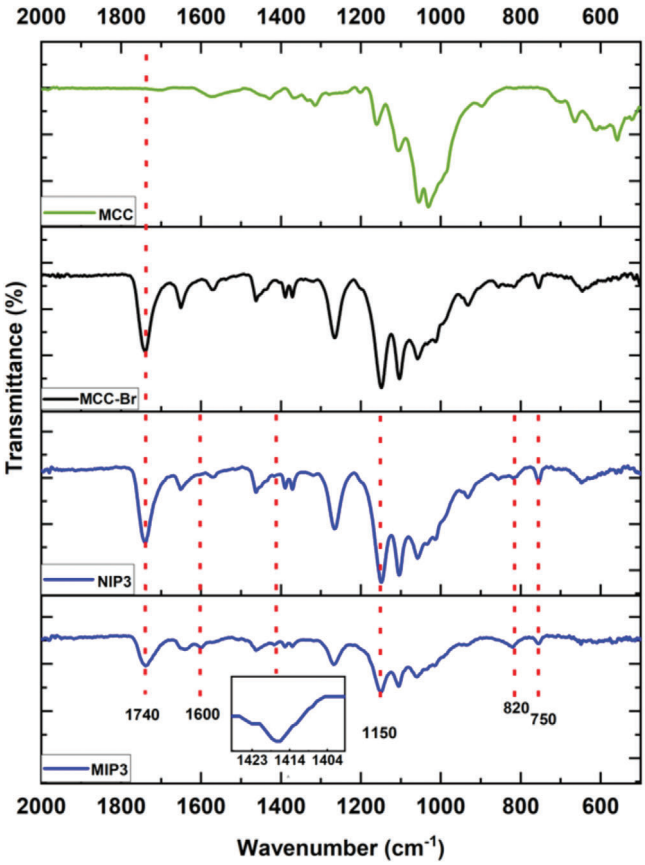

Figure 2. Comparative FTIR spectra for pristine microcrystalline cellulose (MCC), the product resulting from the immobilization of α-bromoisobutyryl bromide in MCC (MCC-Br), NIP3, and MIP3.

as presented in **Figure 2**. Comparing the FTIR spectra for pristine MCC and for the purified MCC-Br product, a new peak at 1740 cm^{-1} is observed in MCC-Br as a consequence of the stretching of the carbonyl group (–C=O) resulting from the reaction between OH groups in cellulose and BIBB (see also Figure 1a). This is the same reaction step also reported in our previous work concerning the grafting of 4VP in MCC without molecular imprinting.[7] Using inductively coupled plasma-mass spectrometry, following our synthesis procedure, the bromide content in MCC-Br is estimated to be of 135 mg g^{-1},[7] which is in a similar range of values reported in the related works.[6]

The general aim of the molecular imprinting is the creation in a polymer network of cavities with stereo-specificity for a selected target compound. For this purpose, functional monomers with potential strong interactions with a template molecule (usually noncovalent interactions such as hydrogen bonding, Van der Waals, π–π staking, etc.) should be selected. Note that in molecular imprinting the template molecule is not necessarily the target compound, as often considered when using a surrogate molecule due to the high price of the target, solubility limitations, etc. After the promotion of the complexation functional monomers–template, a polymerization in the presence of a crosslinking is conducted for molecular cavities formation. The main role of the crosslinker is prompting the creation of binding sites (cavities) with geometrical stability. In spite of the merits of this approach, many factors can weaken the molecular imprinting efficiency, i.e., the formation of a high number of specific binding cavities in the polymer network. Also, the polymerization conditions, namely, the kind and concentrations of all initial components in the reaction mixture (functional monomer(s), template, crosslinker, initiator, solvent(s)), reaction temperature, or initiation mechanism strongly affect the molecular imprinting process.[8]

The purposes of molecular imprinting above described are depicted in Figure 1b for the surface phenomena here seek. A thin synthetic shell with imprinted cavities is intended, via ATRP polymerization, for core cellulose particles. The reaction is made using the macroinitiator MCC-Br particles and the functional monomer 4VP, the template quercetin, the crosslinker EGDMA, and the pair CuBr/*N*,*N*,*N*′,*N*′′,*N*′′-pentamethyldiethylenetriamine (PMDETA) for the ATRP activation/deactivation mechanism. The specific synthesis conditions considered in the molecular imprinting of the surface of the MCC-Br particles via ATRP with 4VP/EGDMA in the presence of quercetin are presented in **Table 1**.

Our goal is the formation of a thin enough imprinted shell in order to enhance binding site accessibility and mass transfer, leading to improved performance of the adsorbent particles in sorption/desorption processes. For that, a low concentration of the monomers 4VP and EGDMA was used, as detailed in Table 1. Note that much higher monomers concentrations lead an eventual to high incorporation of the synthetic copolymer in the MCC particles in view of the present goal. For instance, in the previous work concerning the grafting of 4VP in MCC, with an initial monomer concentration of 5.75 mol L^{-1}, the estimate for the content of the synthetic shell in the final MCC-4VP particles was ≈90 wt%.[7] Under the polymerization conditions presented in Table 1, synthetic shell contents in the range 10% to 20% were estimated (the CuBr and PMDETA concentrations follow usual ATRP ratios after definition of monomers and MCC-Br concentrations).

A too high content of the synthetic shell (depending on the polymerization conditions) and intra/interparticle reaction mechanisms can lead to substantially different materials, namely, concerning their final morphology. In **Figure 3**, possible polymerization reaction mechanisms which are involved in the formation of cellulose-synthetic hybrid particles via ATRP are depicted. Besides the main intraparticle reaction steps for crosslinked shell formation (e.g., propagation of multifunctional active radical centers and reversible activation/deactivation with CuBr), intra- and interparticle radical termination is also possible. The interparticle radical termination can lead to particle connection and eventually to gelation, as observed with our experiments when too concentrated solutions are used.

Due to the high number of different parameters involved in molecular imprinting recipes, although it is possible to use molecular simulation, and/or of experimental design to help with designing tasks,[8] some rules established by solubility constraints, expected thermodynamic effects, and so on, are important for the planning of the experimental runs. Obviously, the selection of the template depends on the application pursued. In this work, quercetin was considered for the molecularly imprinted particles (MIPs) template because it is a flavonoid with

Table 1. Synthesis conditions considered in the surface molecular imprinting of MCC-Br particles considering ATRP of co-monomers 4VP/EGDMA in the presence of quercetin. Polymerization at 70 °C during 72 h.

Material	4VP [× 10^{-3} M]	EGDMA [× 10^{-3} M]	Quercetin [× 10^{-3} M]	MCC-Br [mg mL^{-1}]	CuBr [× 10^{-3} M]	PMDETA [× 10^{-3} M]	DMF [× 10^{-3} M]	ACN [× 10^{-3} M]	Ethanol [× 10^{-3} M]	Synthetic shell [wt%]
MIP1	87.8	17.5	11.0	1.03	1.9	1.9	12796.9	-	-	N.A.
MIP2	73.2	14.6	9.2	0.87	1.6	1.6	10901.8	2839.9	-	19
MIP3	87.4	17.4	6.5	5.15	1.9	1.9	-	-	16898.0	14
MIP4	87.8	17.5	6.5	5.21	1.9	1.9	-	16056.5	2534.6	10

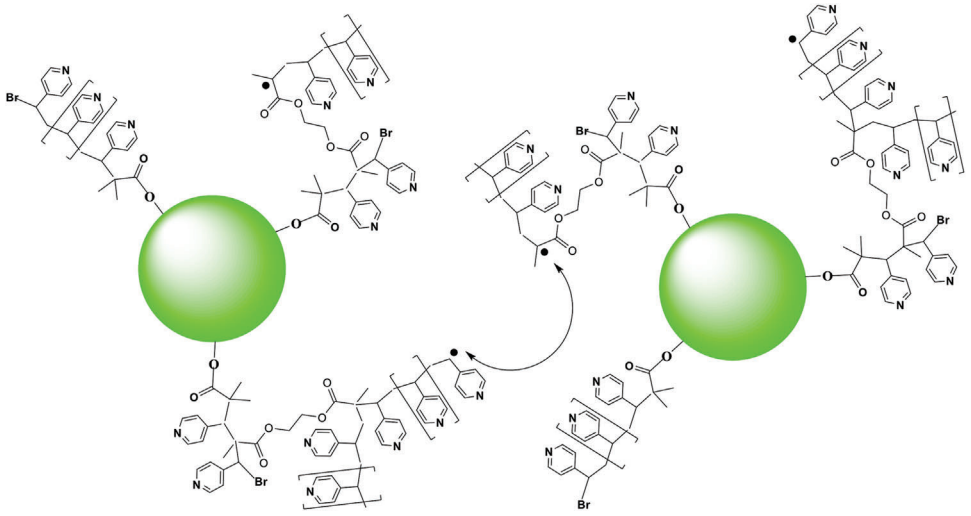

Figure 3. Depiction of possible polymerization reaction mechanisms involved in the surface molecular imprinting of cellulose-synthetic hybrid particles via ATRP. Besides the main intraparticle reaction steps for crosslinked shell formation (e.g., propagation of multifunctional active radical centers and reversible activation/deactivation with CuBr), intra/interparticle radical termination is also possible. The interparticle radical termination can lead to particle connection and eventually to gelation.

a low price (e.g., as compared with luteolin or apigenin), it is reported to be present in olive leaf extracts and contains many interaction points common to other important flavonoids in olive leaf, namely, rutin, luteolin, apigenin, and other related glycosylated compounds. Therefore, quercetin was here considered as a kind of surrogate for the many flavonoids often found in olive leaf extracts. The ratio of functional monomer/template is known to play an important role in imprinting efficiency.[8] However, as pointed before, solubility constraints also define the maximum amount of template that can be used. The concentrations for quercetin in Table 1 are a consequence of that kind of analysis for the present MIPs synthesis runs.

Hydrogen bonding capacity and polarity of the solvent have a strong influence in polymerization mechanisms and particular additional issues are observed with molecular imprinting polymerization systems. Potential interference with the interactions expected between functional monomer(s)-template and lack of initial solubility for all polymerization ingredients are factors constraining the selection of the working solvent. Our studies included the change of the polymerization solvent(s) as presented in Table 1, going from dimethylformamide (DMF, highly polar and allowing higher solubilization of ingredients), mixtures with ACN (acetonitrile presents a lower H-bonding capacity but causes solubility problems with the reaction mixtures) and ethanol (presenting H-bonding effects but allowing a higher solubilization effect).

The selection of 4VP as functional monomer was driven by previous results concerning the development of MIPs for different kinds of polyphenols.[8–12] Indeed, 4VP can establish a strong binding with polyphenols, even at low extent of hydrophobic effects, due to the particular features for the –N= group in the pyridyl moiety. Specifically, one extra electron pair that is not involved in the ring conjugation system that is able to participate in strong H-bonding mechanisms, as well as to bind with protons. The pyridyl group behaves as a proton acceptor (small nucleophilic molecule that can interact with exposed electrophilic residues), being also a good ligand for multiple metal ions, giving rise to complexation. Due to these particular properties, polymers based on 4VP are being considered for heavy metals ions adsorption and wastewater/industrial effluents treatment,[13–17] enzymes/protein adsorption,[18,19] and other applications involving electronics, biomedicine, or catalysis.[20]

Experimental runs reported in Table 1 lead to products with different features concerning synthetic functionalization and morphology, impacting their use with sorption/desorption processes. With the product MIP1, a kind of solubilization of the macroinitiator MCC-Br particles was observed during polymerization. Under our working conditions, using DMF solvent makes the ATRP

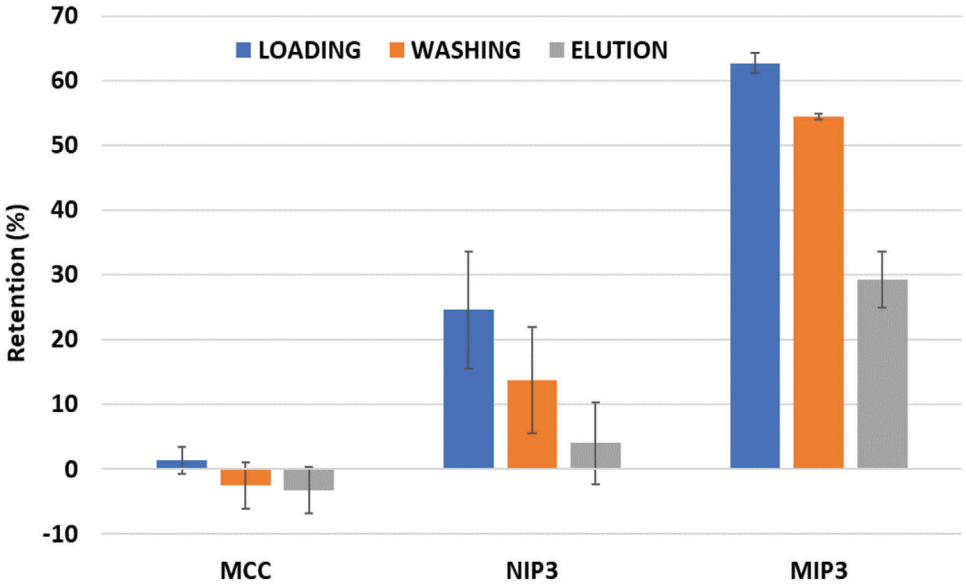

Figure 4. Fraction of the initial amount of quercetin retained in pristine MCC, NIP3, and MIP3 after the loading, washing, and elution steps in SPE. Testing ($n = 2$) using a quercetin solution in ethanol/water 80/20 with concentration 0.126×10^{-3} M, 2.5 mL of volume of liquid phase in each step, and 25 mg of adsorbent in the SPE cartridges. Estimates with UV measurements at 370 nm.

step close to a homogenous process and the size of the final particles is too low to allow the practical use of the material as an adsorbent. A favorable morphology was observed with MIPs 2 to 4 but the FTIR analysis of the products indicates a clearer functionalization of the materials with 4VP for MIP3, as shown in Figure 2 (see Supporting Information for FTIR analysis of MIPs/nonimprinted particles (NIPs) 1, 2, and 4). Characteristic peaks for 4VP monomer at 1600 cm^{-1} (C=C pyridyl), 1418 cm^{-1} (C=N), 820 and 755 cm^{-1} (both correspond to the C–H bending in the pyridine ring) are all potential indicators for incorporation of this monomer, particularly the 1418 cm^{-1} assignment. Note that, in comparison with other works,[8–12] a weaker signal for these 4VP peaks is here expected due to the lower incorporation of this monomer in the final products. The presence of EGDMA in polymer materials is usually confirmed by analyzing assignments at 1720 and 1130 cm^{-1} (C=O and C–O groups, respectively). Peaks close to these vibrational regions are observed in all synthesized products but an important contribution of similar functional groups in MCC-Br is possible (note the relatively small concentration of EGDMA is used here).

Overall, with ethanol as ATRP solvent, a solid/liquid heterogenous process was observed along the reaction, preserving a final size of the hybrid particles suitable for their application as adsorbent. The incorporation of the 4VP/EGDMA co-monomers, apparent in FTIR analysis, indicated the MIP3 particles as good candidates for testing with selective sorption/desorption, as explored in the next sections.

2.2. Sorption/Desorption Assessment with Standard Polyphenols

To evaluate the surface modification achieved in the pristine MCC, specifically concerning sorption capacity for phenolic compounds due to synthetic shell formation and also to assess the benefits of molecular imprinting, solid phase extraction (SPE) testing for MIP/NIP3 was performed with standard compounds, namely, the flavonoid quercetin (the imprinting template), rutin (a glycoside of quercetin often found in olive leaf), vanillic acid (a phenolic acid also reported in olive leaf extracts), and the oleuropein secoiridoid, that is the most abundant compound in olive leaf. In order to approach practical industrial working conditions with olive leaf extracts, ethanol/water 80/20 was used as solvent in these studies.

Results presented in **Figure 4** put into evidence a very low retention capacity for quercetin of pristine cellulose while the amount retained by NIP3 and MIP3 in the loading step is much higher (more than 60% with the MIP). Clearly, these outcomes show the modification achieved for the cellulose surface and the active role of the 4VP/EGDMA shell in quercetin binding, namely, due to the interaction with 4VP. Moreover, the quercetin retention observed with MIP3 (≈62.7 %) is also much higher than with NIP3 (≈24.5 %), highlighting the benefits of molecular imprinting. An imprinting factor IF ≈2.6 is estimated based on these measurements. Furthermore, the comparison of the results for NIP3 and MIP3 concerning the washing and elution steps show also the higher strength for the binding of quercetin with MIP3 comparatively to NIP3. These measurements are additional confirmations for the creation of specific binding sites in MIP3 due to molecular imprinting.

Measurements presented in **Figure 5** show a low retention of oleuropein in MIP3 comparatively to quercetin. This difference can be explored to make the separation between flavonoids and secoiridoids in olive leaf. Rutin and vanillic acid, especially the latter, are retained at a large extent in MIP3. This is a consequence of binding effects that are inevitable when the compounds bear functional groups similar to that we used to promote the interaction of the template with the functional monomer or other that are able to interact with polymer network.

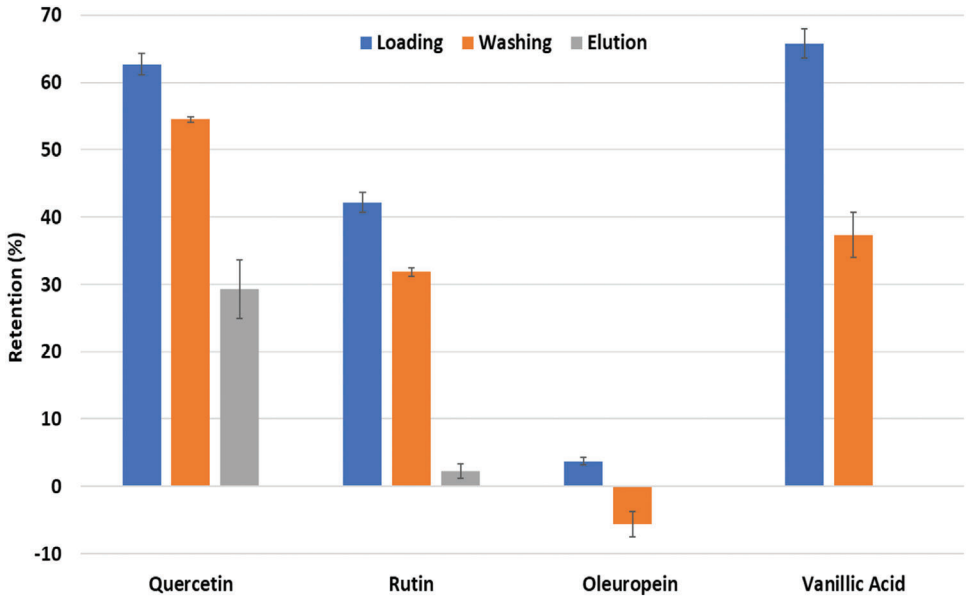

Figure 5. Fraction of the initial amount of standard compound's quercetin, rutin, oleuropein, and vanillic acid retained in MIP3 after the loading, washing, and elution steps in SPE. Testing ($n = 2$) using solutions of the different standards in ethanol/water 80/20 with concentration 0.126×10^{-3} M, 2.5 mL of volume of liquid phase in each step, and 25 mg of adsorbent in the SPE cartridges. Estimates with UV measurements at 370 nm for quercetin and rutin and at 280 nm for vanillic acid and oleuropein.

For instance, rutin contains phenolic OH groups that are also able to interact with the 4VP/EGDMA network. Also, vanillic acid contains a phenolic OH and a carboxylic group that can bind with the pyridine moieties. Due to its smaller size, vanillic acid should also have a facilitated access to the binding sites. However, the later washing and elution steps clearly show the high binding strength of quercetin with MIP3. Note that vanillic acid is totally desorbed from the MIP in the elution step with methanol/acetic acid 90/10 (see Section *Sorption/Desorption Experiments with Polyphenol Standards* for experimental details). These results also highlight the possibility for the use of MIP3 to make the fractionation of complex olive leaf extracts through designed sorption/desorption processes.

2.3. Enrichment of Flavonoids in Olive Leaf

Olive leaves are being considered with increasing interest as a source of bioactive compounds, including antioxidants, to be used in food (e.g., supplements with health-giving effects), natural preservatives, cosmetics, among other applications. Many of these bioactive compounds in olive leaf are phenolic molecules belonging to different classes, ranging from simple phenols and phenolic acids, secoiridoids, lignans, and flavonoids. For instance, the simple phenyl alcohols tyrosol and hydroxytyrosol and the phenolic acids gallic acid and vanillic acid are commonly found in olive leaf. Oleuropein, a secoiridoid, is the main phenolic component in olive leaves but many other compounds belonging to this family are also observed, while pinoresinol is a lignan reported in this context. Diverse kinds of flavonoids are present in olive leaf, namely, the aglycones quercetin, luteolin, apigenin, and diosmetin and the related glycosylated forms such as luteolin-7-O-glucoside, luteolin-5-O-glucoside, luteolin-7-O-rutinoside, quercetin-7-O-rutinoside, rutin, or apigenin-4′-glucoside.

The relative distribution and amounts of these different phenolic compounds in olive leaf depend on the tree variety, geographical origin, and collection season. Furthermore, the extraction technique used to get these molecules impacts on the composition of the final extract. Commonly used methods rely on solid/liquid extraction with hydroalcoholic solvent mixtures (e.g., ranging from pure water to pure ethanol or methanol), ethyl acetate, acetone, or even dichloromethane (or similar solvents when the nonpolar fraction is sought). Many studies addressed the effect of the extraction technique on phenolic profile and a dependence for the yield of the different phenolic compounds is known.[21–32] Anyway, at the end, extracts containing a huge diversity of compounds are obtained, thus demanding separation and purification steps to get individual molecules or mixtures suitable for practical applications (e.g., in food supplements or cosmetics). Here, the testing of the developed surface imprinted adsorbents for the fractionation of an industrial olive leaf extract is highlighted. **Figure 6** shows the high-performance liquid chromatography with diode-array detection (HPLC-DAD) analysis of this extract showing a major peak for oleuropein (Figure 6a) but many other compounds are observed, including different kinds of flavonoids in the aglycone form (quercetin, luteolin) or glycosylated (e.g., luteolin-7-O-glucoside, as clearly shown in Figure 6b). Verbascoside, phenolic acids, and phenyl alcohols are also identified, among a plethora of minority compounds (see the huge diversity in the magnified views, Figure 6c,d). This tentative identification task was also aided by liquid chromatography-mass spectrometry (LC-MS) analysis, as described in the Experimental Section.

Figure 7 shows the dynamics of sorption of this olive leaf industrial extract in the MIP3 particles for one of the runs per-

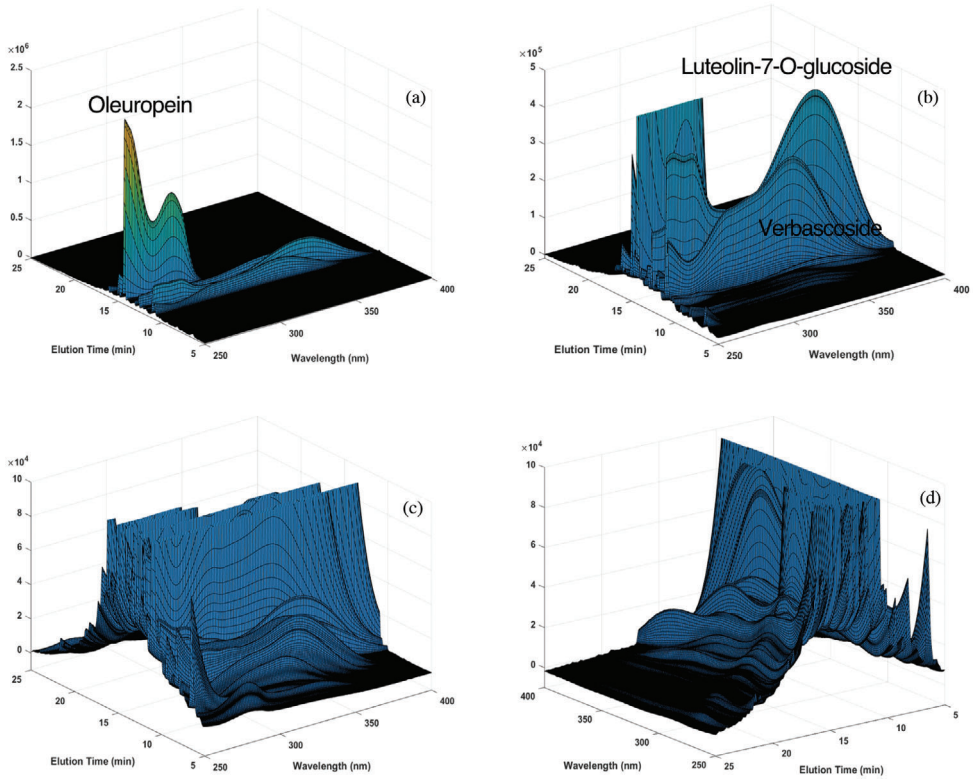

Figure 6. HPLC-DAD chromatogram for the olive leaf extract provided by NATAC that was used in this work. a) full view of the chromatogram. b–d) Magnified views of this chromatogram to highlight the compositional complexity of the extract.

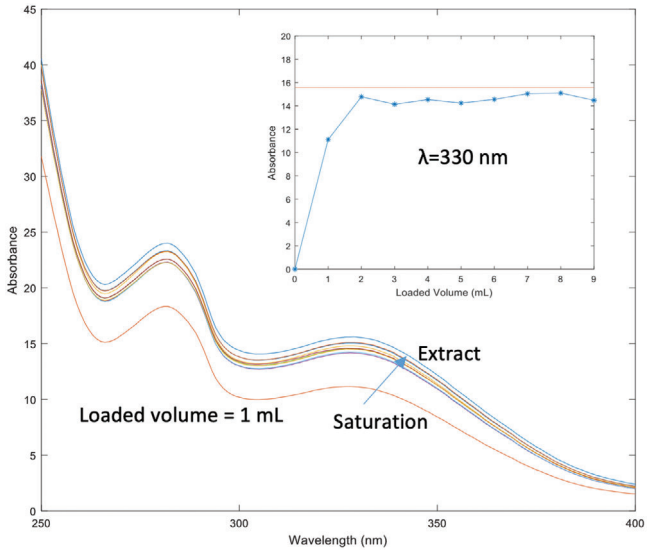

Figure 7. Dynamics for the SPE sorption of the olive leaf extract in ethanol/water 80/20 at $C = 5$ mg mL^{-1} using 25 mg of MIP3. The UV-vis analysis of samples collected at SPE column outlet for different loading volumes show the dynamics observed with particles saturation (approaching the extract spectrum). The inset shows the sorption dynamics measured at $\lambda = 330$ nm (breakthrough curve).

formed here. Note that these breakthrough curves are affected by a competitive adsorption phenomenon involving the different compounds present in the olive leaf extract and the available binding sites. However, due to the 4VP functionalization of the adsorbent and imprinting with quercetin, a preferential sorption of flavonoids is expected. Therefore, for instance, the displacement of previously adsorbed secoiridoids by flavonoids is possible during this dynamic process. Hydroalcoholic mixtures with high alcohol content were considered in our loading runs. This is possible due to the strong binding capacity of 4VP for flavonoids even with low water content solvents, as shown previously.[7–12] Therefore, a higher efficiency is possible due to the feasibility for the processing of industrial extracts produced in alcoholic solvents with a minimum of preparation steps.

Figure 8 presents the 2D HPLC-DAD chromatograms for different fractions collected during the desorption of MIP3 particles preloaded with the olive leaf extract in ethanol/water 50/50 at a concentration of 5 mg mL^{-1}. Measurements at 280 and 330 nm are presented to highlight the fractionation of flavonoid and nonflavonoid compounds. A full view for selected fractions produced along this desorption process is presented in **Figure 9**. These results highlight the performance of the developed MIP particles for compounds separation due to the different binding strengths. Key compounds such as oleuropein, verbascoside, oleuroside, luteolin-7-O-glucoside, apigenin-7-O-glucoside, luteolin-4-O-glucoside, diosmetin-4-O-glucoside, and quercetin are considered to illustrate these aspects. The fraction recovered

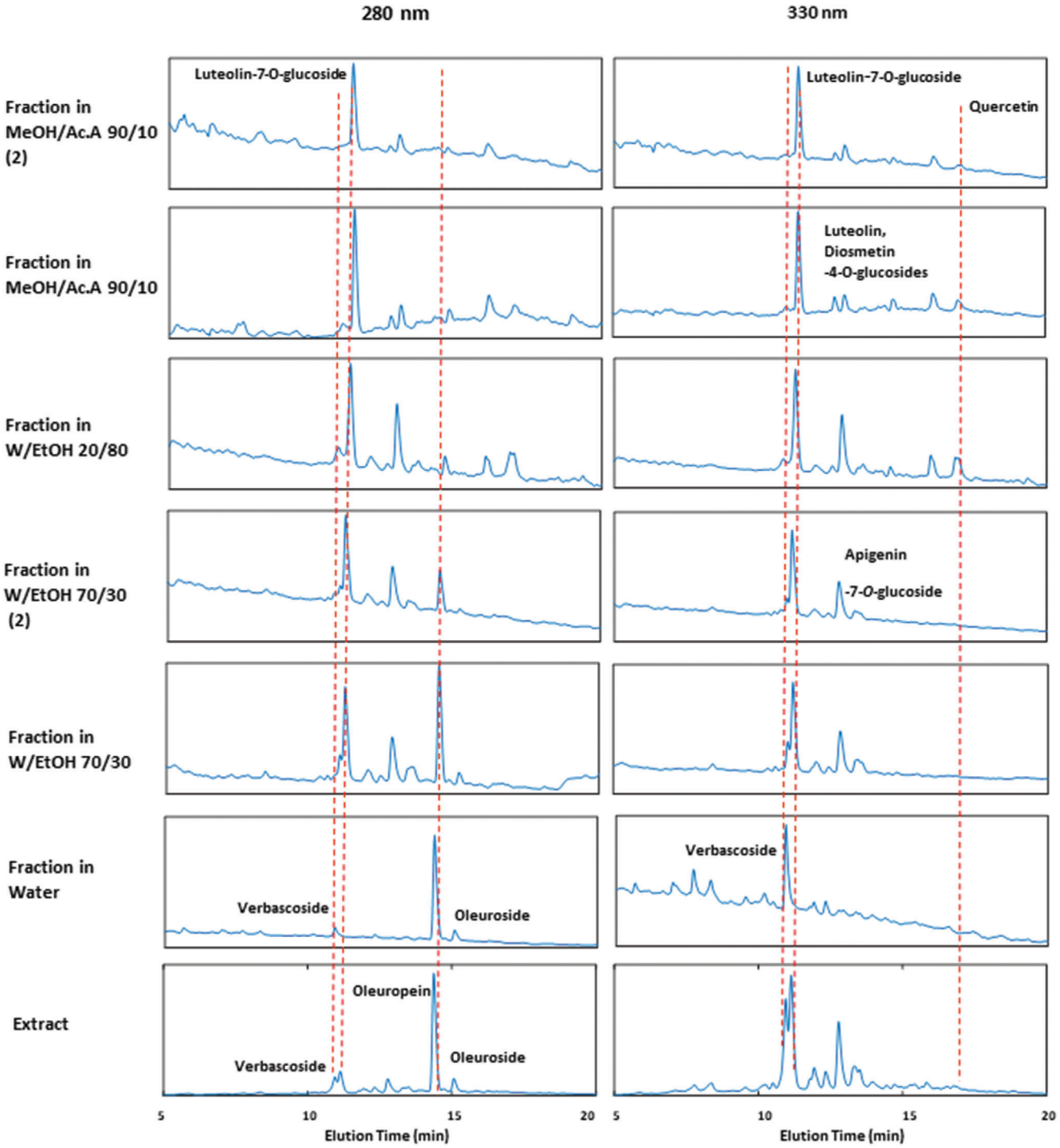

Figure 8. 2D HPLC-DAD chromatograms for different fractions collected during the desorption of MIP3 particles preloaded with the olive leaf extract in ethanol/water 50/50 at 5 mg mL^{-1}. Measurements at 280 and 330 nm are presented to highlight the fractionation of flavonoid and nonflavonoid compounds. For graphical simplicity, numerical scales in the plots were omitted.

in water (see Figures 8 and 9a) is enriched with oleuropein, verbascoside, and oleuroside comparatively to the initial extract. Under these desorption conditions, flavonoids keep retained in the MIP particles. When the alcoholic content in the elution solvent is increased, some flavonoids such as luteolin-7-O-glucoside and apigenin-7-O-glucoside start to desorb and fractions with mixed composition flavonoid/nonflavonoid are obtained. Only when the elution strength of the solvent is substantially increased (e.g., water/ethanol 20/80 or methanol/acetic acid 90/10), the compounds with strong binding to the MIP sites can be recovered. This is observed with luteolin-4-O-glucoside, diosmetin-4-O-glucoside, and quercetin (the template of the

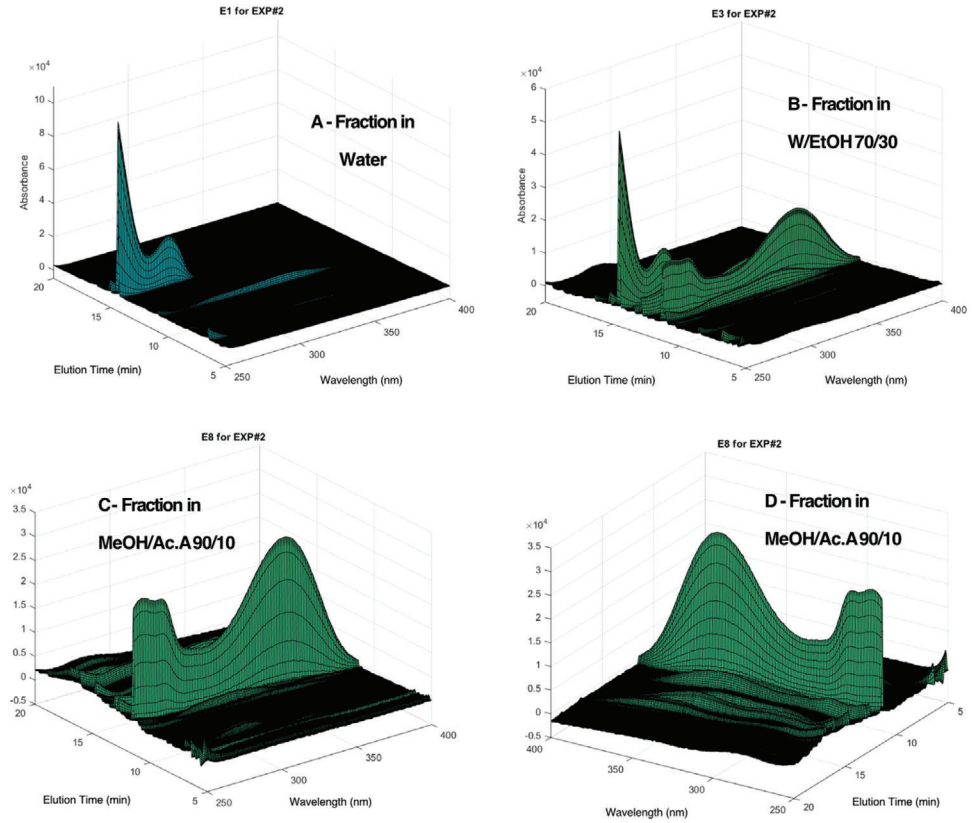

Figure 9. 3D HPLC-DAD chromatograms for different fractions collected during the desorption of MIP3 particles preloaded with the olive leaf extract in ethanol/water 50/50 at 5 mg mL^{-1}. a) Fraction recovered in water showing the enrichment of oleuropein. b) Fraction recovered in water/ethanol 70/30 showing the increase of flavonoids content, namely, luteolin-7-O-glucoside. c) Fraction recovered in methanol/acetic acid 90/10 showing a high enrichment in flavonoids, namely, luteolin-7-O-glucoside and other minority related compounds. d) A different view of the same flavonoid-enriched fraction.

MIP). As a consequence, fractions with high flavonoid content can be obtained, as presented in Figures 8 and 9c,d.

HPLC-DAD results were used to estimate the enrichment factors achieved for the production fractions resulting from this sorption/desorption approach. The global enrichment factor for flavonoids was estimated from EF = $(A_{360}/A_{280})_F/(A_{360}/A_{280})_E$ with EF representing the enrichment factor and $(A_{360}/A_{280})_F$ the ratio of the chromatogram areas at 360 and 280 nm for the fraction in analysis and $(A_{360}/A_{280})_E$ the same ratio observed in the extract. Our measurements show to be possible to achieve EF up to four times, as presented in **Table 2** and complemented with Figure 9 and similar graphs presented in the Supporting Information (Figures S4–S9, Supporting Information).

It is also worth to highlight the superior performance of MIP3 versus NIP3 concerning the enrichment of flavonoids in olive leaf extracts. **Figure 10** presents the comparison for 2D HPLC-DAD chromatograms for a fraction collected during the desorption of MIP3 and NIP3 particles preloaded with the olive leaf extract in ethanol/water 50/50 at 5 mg mL^{-1}. These results clearly show the higher selectivity of MIP3 toward flavonoids, namely, quercetin, in comparison with NIP3. These outcomes highlight the importance of the binding sites created through the presence of quercetin in the polymerization system, besides the strong interaction between the moieties of 4VP and flavonoid molecules.

Table 2. Enrichment factors (EFs) for total flavonoids and quercetin estimated for different fractions recovered with MIP3 particles after processing of an olive leaf extract considering different working conditions.

Processed extract solution	Solvent in the recovered fraction	EF for flavonoids	EF for quercetin
EtOH/W 50/50 at $C = 5$ mg L^{-1}	Water	-	-
	EtOH/W 70/30	1.6	-
	MeOH/Ac.A 90/10	2.7	3.5
EtOH/W 80/20 at $C = 0.5$ mg L^{-1}	MeOH/Ac.A 90/10	2.0	-
EtOH/W 80/20 at $C = 5$ mg L^{-1}	Water	-	-
	EtOH/W 30/70	2.8	-
	EtOH/W 50/50	3.5	-
	EtOH/W 80/20	3.8	-
	MeOH/Ac.A 90/10	3.7	2.6

Additional information is presented in the Supporting Information concerning the results for fractions resulting from the processing of the olive leaf extract in ethanol/water 80/20 at 0.5 mg mL^{-1} and ethanol/water 80/20 at 5 mg mL^{-1}. Purification achieved with these working conditions demonstrate the ability of the developed adsorbents to perform in a wide range of context

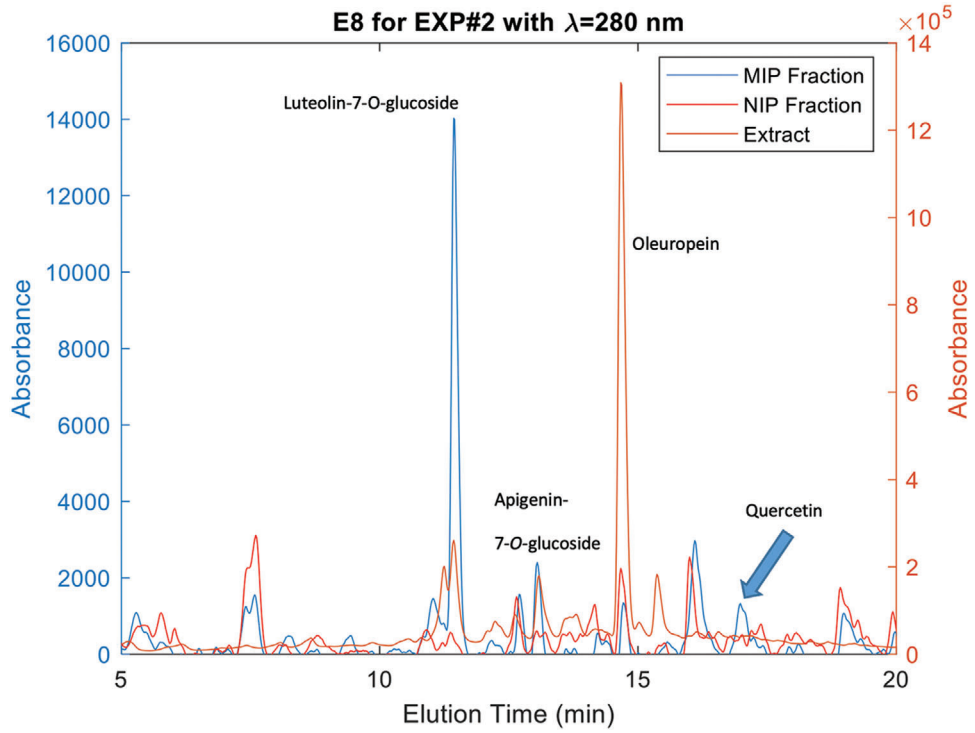

Figure 10. 2D HPLC-DAD chromatograms for a fraction collected during the desorption of MIP3 and NIP3 particles preloaded with the olive leaf extract in ethanol/water 50/50 at 5 mg mL^{-1}. Fraction recovered in methanol/acetic acid 90/10 showing the high selectivity of MIP3 toward flavonoids, namely, quercetin, in comparison with NIP3.

Table 3. Productivity data estimated for different fractions resulting from the processing of olive leaf extracts with the hybrid cellulose-synthetic MIP3 particles.

Sorption conditions	Desorption fraction	Productivity [mg compound g^{-1} adsorbent]					
		Oleuropein	Verbascoside	Oleuroside	Luteolin-7-O-glucoside	Apigenin-7-O-glucoside	Quercetin
EtOH/W 50/50 at $C = 5$ mg L^{-1}	Water	3.01	0.15	0.32	-	-	-
EtOH/W 50/50 at $C = 5$ mg L^{-1}	W/EtOH 70/30	1.62	0.07	0.15	0.18	0.10	-
EtOH/W 50/50 at $C = 5$ mg L^{-1}	MeOH/Ac.A 90/10	0.02	0.01	0.02	0.20	0.05	0.05
EtOH/W 50/50 at $C = 5$ mg L^{-1}	MeOH/Ac.A 90/10	-	-	-	0.06	0.02	-
EtOH/W 80/20 at $C = 5$ mg L^{-1}	W/EtOH 50/50	0.01	-	-	0.20	0.01	0.02
EtOH/W 80/20 at $C = 5$ mg L^{-1}	MeOH/Ac.A 90/10	-	-	-	0.13	0.02	-

concerning solvent composition and solute concentration. Previous studies addressing the development of MIP particles for the purification of olive leaf extracts consider the processing of ethyl acetate solutions with oleuropein as target compound[32] or considered operation with standard compounds.[33] Here, we propose the use of the hybrid MIP particles for the fractionation of hydro-alcoholic industrial extracts with production of enriched flavonoids fractions but also oleuropein-enriched mixtures, as discussed above.

Table 3 presents the productivity data estimated for different fractions resulting from the processing of olive leaf extracts with the hybrid cellulose-synthetic MIP3 particles. Productivity parameter is defined as the amount of a specific compound produced in a given fraction per unit of mass of the MIP adsorbent particles. These values are estimated from the HPLC-DAD analysis of the fractions (see, e.g., Figures 8 and 9 and Supporting Information) and the HPLC-DAD calibration data for different standard compounds (e.g., oleuropein, verbascoside, luteolin-7-O-glucoside, quercetin, etc.).

Complementary to results in Table 2, the data in Table 3 confirm the usefulness of the developed MIP particles for compounds fractionation. Indeed, higher amounts of secoiridoids and related compounds are produced in the aqueous fractions while higher flavonoids productivity is observed for organic fractions (e.g., MeOH/Ac.A 90/10). These outcomes indicate the developed natural-synthetic materials as promising adsorbents to

be considered with cyclic sorption/desorption processes aiming at to get high-added value compounds in olive leaf.

3. Conclusions

Surface molecularly imprinted cellulose-synthetic hybrid particles were prepared via ATRP with quercetin as template and used in sorption/desorption processes involving standard phenolic compounds as well as olive leaf extracts. The later are complex mixtures of flavonoid and nonflavonoid compounds (e.g., oleuropein). These testing runs evidenced the higher performance of the molecularly imprinted particles, not only in comparison with the native cellulose, but also in contrast with the nonimprinted hybrid materials. The quercetin-shaped imprinted cavities and the strong interaction between 4VP moieties and flavonoids were explored for the enrichment of olive leaf extracts through sorption/desorption processes with the developed particles. We show that hydro-alcoholic solvent mixtures with high alcoholic content can be considered for the processing of the olive leaf extracts with the new MIP particles. The production of rich fractions containing luteolin-7-O-glucoside, apigenin-7-O-glucoside, or quercetin, among other flavonoids was demonstrated through this approach. Enrichment factors up to four times were estimated for some fractions produced.

Next steps in this research line include the mass-production of these kind of particles, intending to approach the industrial scale for the efficient valorization of target compounds biomass contained, in the framework of circular bio-economy.

4. Experimental Section

Materials: All chemicals were used as purchased, without further purification. Microcrystalline cellulose (MCC, powder, 20 µm, cotton linters), BIBB (98% purity), triethylamine (TEA, 99.5% purity), 4-(dimethylamino)pyridine (DMAP, purity≥ 99%), CuBr (97% purity), and PMDETA (99% purity) were purchased from Sigma-Aldrich. 4-vinylpyridine (4VP, 95% purity) was provided by Alfa Aesar. Analytical reagent grades for ACN, DMF, acetic acid (AcOH), and methanol (MeOH) were bought from Fisher Scientific and for ethanol (EtOH) from PanReac. Quercetin (hydrate, purity 95%) and rutin (purity 97%) were supplied by Acros Organics. Oleuropein (pure) was purchased from PanReac and vannilic acid (purity 97%) from Sigma-Aldrich. These standard polyphenols were used in the synthesis and testing of the materials here addressed. The water used in the experiments was ultrapure water supplied by the local laboratory.

Immobilization of BIBB in MCC: The immobilization of BIBB in MCC was performed using the reported esterification procedure, as described previously.[7] Briefly, in a typical experiment, 1 g of MCC was dispersed in DMF (100 mL) using sonication. Then, triethylamine (8 mL) and DMAP (4 g) were added to the MCC dispersion and, afterward, BIBB (8 mL) was dropwise fed to the suspension at 0 °C. The reaction was allowed to proceed at room temperature during 24 h. At the end, ethanol was used to terminate the esterification. Products were washed with DMF until the achievement of a colorless liquid phase and then ATRP macroinitiator MCC-Br was purified using dialysis (3.5k MWCO, ThermoFisher Scientific dialysis bag) with deionized water, followed by drying in vacuum oven at 40 °C.

Surface Imprinting in MCC-Br Macroinitiator Particles via ATRP: The required amounts of dried ATRP macroinitiator MCC-Br, functional monomer 4VP, and template quercetin were added to the polymerization solvent and the interaction functional monomer-template was promoted in an ultrasounds ice bath during 30 min. Then, the remaining reactants (EGDMA, CuBr, and PMDETA) were dissolved in that solution and a flow of dry argon was used to purge the mixture for 30 min. Afterward, polymerization took place in a sealed vessel during 72 h at 70 °C. The final polymerization products were purified in 3.5k MWCO dialysis bags with successive changing of the methanol/acetic acid 90/10 cleaning solvent. In parallel to the above-described synthesis procedure for surface MIPs, NIPs were prepared by avoiding the presence of quercetin. The purified MIPs and NIPs were dried in vacuum oven at 40 °C up to the measurement of a constant weight. Gravimetric analysis was considered to estimate the amount of synthetic polymer in the final hybrid MCC particles.

Products Characterization using FTIR Spectroscopy: Purified and dried products were characterized through FTIR spectroscopy with a Perkin Elmer, model Spectrum Two, instrument. These analyses were directly performed in ATR mode or, when needed, polymers were mixed with KBr and pressed into pellets in order to collect the correspondent IR spectra.

HPLC-DAD Analysis: An HPLC system (KNAUER) consisting of a gradient pump (P6.1 L) equipped with a degasser, an autosampler (6.1 L), a column thermostat (CT2.1), and a DAD (6.1 L) was used in this research. ClarityChrom was the software allowing the control of the HPLC system. The chromatographic analysis was performed using an Ascentis C18 (SUPELCO) column with a particle size of 5 µm and dimensions 25 cm × 4.6 mm. A gradient of solvents was used as a mobile phase varying from 100% of water-ACN (9:1) to 100% water-ACN (1:9) for 45 min. The mobile phase water pH was adjusted to 3 using acetic acid. The flow rate of the chromatographic analyses was 1 mL min^{-1}, and the temperature of the column was set at 45 °C.

Identification and Quantification of Polyphenols in Olive Leaf Extracts using LC-DAD-ESI-MS^n: These analyses were carried out at the Centro de Investigação de Montanha (CIMO). The chromatographic analysis was performed using a Dionex UltiMate 3000 UPLC (Thermo Scientific, San Jose, CA, USA) system equipped with a diode array detector coupled to an electrospray ionization mass detector (LC-DAD-ESI/MS^n), a quaternary pump, an auto-sampler, a degasser, and an automated thermostatic column compartment. Chromatographic separation was carried out with a Waters Spherisorb S3 ODS2(C18), L × I.D. = 15 cm × 4.6 mm and 3 µm particle column (Waters, Milford, MA, USA) working at 35 °C. The solvents used were: A) 0.1% formic acid in water, B) acetonitrile. The elution gradient established was isocratic 15% B (5 min), 15% B to 20% B (5 min), 20–25% B (10 min), 25–35% B (10 min), 35–50% B (10 min), and re-equilibration of the column, using a flow rate of 0.5 mL min^{-1}.

UV/Vis Spectroscopy: A spectrophotometer P9 Double Beam UV-Visible, VWR, was used for fast assessment of cleaning steps, breakthrough curves, and quantification of simple polyphenol solutions, namely, with the loading, washing, and elution steps for the assessment of MIPs/NIPs sorption/desorption with polyphenol standards.

Sorption/Desorption Experiments with Polyphenol Standards: Assessment of the sorption/desorption capabilities of the MIPs/NIPs was performed with 25 mg of the dry materials in SPE packing cartridges (Agilent Bond Elut reservoir, 1 mL capacity). Adsorbents were first cleaned (successive loading and elution steps using methanol/acetic acid 90/10 with UV/vis monitoring) and afterward conditioned with the desired testing solvent (e.g., ethanol/water 80/20), during at least 24 h before use. Cartridges were then loaded with 2.5 mL of the selected polyphenol solution at concentration 0.126×10^{-3} M considering typically 15 min for total percolation time. The adsorbed polyphenol profile was quantified through UV/vis analysis of the liquid collected at column outlet. The washing desorption step was performed by percolating the same volume of clean solvent through the adsorbent particles and, afterward, the elution desorption step was made with the same volume of methanol/acetic acid 90/10. Desorbed amounts of polyphenol were quantified also by UV/vis analysis of the collected liquid phases in the washing and elution desorption steps.

Sorption/Desorption Experiments with Olive Leaf Extracts: An industrial olive leaf extract provided by NATAC (Alcorcón, Madrid, Spain) was used along these experiments. The required amount of solid olive leaf extract was dissolved in the selected solvent (e.g., ethanol/water 80/20) to meet the target concentration (e.g., 5 mg mL^{-1}). Breakthrough curves were assessed with the adsorbent particles in SPE cartridges, as described above. Fixed volumes of the extract solution (e.g., 2.5 mL) were percolated through the particles and the liquid phase at column outlet was analyzed

by UV/vis spectroscopy to evaluate the sorption process. After saturation, predefined desorption steps were performed with fixed volumes of successive different solvents (e.g., from pure water to pure ethanol). Samples collected at column outlet for each desorption step were analyzed by HPLC-DAD for evaluation of olive leaf extract fractionation and enrichment of target compounds.

Supporting Information

Supporting Information is available from the Wiley Online Library or from the author.

Acknowledgements

The authors acknowledge the support through the OLEAF4VALUE project. This project had received funding from the Bio-Based Industries Joint Undertaking under the European Union's Horizon 2020 research and innovation programme under grant agreement no. 101023256. C.G. acknowledges FCT for the Ph.D. scholarship 2020.06057.BD. The authors also thank NATAC for providing the olive leaf extracts and the aid with the identification by LC-MS of compounds there contained. R.D. is grateful to the Foundation for Science and Technology (FCT, Portugal) for financial support through national funds FCT/MCTES (PIDDAC) to CIMO (UIDB/00690/2020 and UIDP/00690/2020) and SusTEC (LA/P/0007/2020). M.R.C. acknowledges the support by LA/P/0045/2020 (ALiCE), UIDB/50020/2020, and UIDP/50020/2020 (LSRE-LCM), funded by national funds through FCT/MCTES (PIDDAC).

Conflict of Interest

The authors declare no conflict of interest.

Data Availability Statement

The data that support the findings of this study are available from the corresponding author upon reasonable request.

Keywords

adsorbents, atom transfer radical polymerization, cellulose, natural-synthetic hybrid particles, olive leaf, surface molecular imprinting, flavonoids

Received: January 31, 2023
Revised: March 6, 2023
Published online: March 25, 2023

[1] OLEAF4VALUE, https://oleaf4value.eu (accessed: January 2023).
[2] P. Pérez-Larrán, B. Díaz-Reinoso, A. Moure, J. L. Alonso, H. Domínguez, *Curr. Opin. Food Sci.* **2018**, *23*, 165.
[3] C. Dong, H. Shi, Y. Han, Y. Yang, R. Wang, J. Men, *Eur. Polym. J.* **2021**, *145*, 110231.
[4] A. Carlmark, E. E. Malmström, *Biomacromolecules* **2003**, *4*, 1740.
[5] X. Sui, J. Yuan, M. Zhou, J. Zhang, H. Yang, W. Yuan, Y. Wei, C. Pan, *Biomacromolecules* **2008**, *9*, 2615.
[6] Z. Zhang, X. Wang, K. C. Tam, G. Sèbe, *Carbohydr. Polym.* **2019**, *205*, 322.
[7] C. P. Gomes, R. C. S. Dias, *React. Funct. Polym.* **2021**, *164*, 104930.
[8] A. Bzainia, R C. S. Dias, M. R. P. F. N. Costa, *Macromol. React. Eng.* **2023**, 2200076.
[9] C. Gomes, G. Sadoyan, R. Dias, M. Costa, *Processes* **2017**, *5*, 72.
[10] C. P. Gomes, R. C. S. Dias, M. R. P. F. N. Costa, *Chromatographia* **2019**, *8*, 893.
[11] C. P. Gomes, V. Franco, R. C. S. Dias, M. R. P. F. N. Costa, *Chromatographia* **2020**, *83*, 1539.
[12] A. Bzainia, R. C. S. Dias, M. R. P. F. N. Costa, *Molecules* **2022**, *27*, 6406.
[13] Y. Chen, W. Zhao, J. Zhang, *RSC Adv.* **2017**, *7*, 4226.
[14] E. S. Yanovska, L. O. Vretik, O. A. Nikolaeva, Y. Polonska, D. Sternik, O. Yu. Kichkiruk, *Nanoscale Res. Lett.* **2017**, *12*, 217.
[15] C. Xiao, J. Lin, *ACS Omega* **2020**, *5*, 23099.
[16] Y. A. B. Neolaka, Y. Lawa, J. N. Naat, A. A. Pau Riwu, H. Darmokoesoemo, G. Supriyanto, C. I. Holdsworth, A. N. Amenaghawon, H. S. Kusuma, *React. Funct. Polym.* **2020**, *147*, 104451.
[17] N. Amaly, Y. Ma, A. Y. El-Moghazy, G. Sun, *Sep. Purif. Technol.* **2020**, *250*, 117086.
[18] M. Atif, C. Chen, M. Irfan, F. Mumtaz, K. He, M. Zhang, L. Chen, Y. Wang, *Eur. Polym. J.* **2019**, *120*, 109199.
[19] N. Sahiner, O. Ozay, *React. Funct. Polym.* **2011**, *71*, 607.
[20] O. Ghomari, F. Sounni, Y. Massaoudi, J. Ghanam, L. B. Drissi Kaitouni, M. Merzouki, M. Benlemlih, *Biotechnol. Rep.* **2019**, *23*, e00347.
[21] N. Talhaoui, A. M. Gómez-Caravaca, L. León, R. De La Rosa, A. Segura-Carretero, A. Fernández-Gutiérrez, *LWT–Food Sci. Technol.* **2014**, *58*, 28.
[22] M. Laguerre, L. J. L. Giraldo, G. Piombo, M. C. Figueroa-Espinoza, M. Pina, M. Benaissa, A. Combe, A. Rossignol Castera, J. Lecomte, P. Villeneuve, *J. Am. Oil Chem. Soc.* **2009**, *86*, 1215.
[23] A. L. S Oliveira, S. Gondim, R. Gómez-García, T. Ribeiro, M. Pintado, *J. Environ. Chem. Eng.* **2021**, *9*, 106175.
[24] N. Talhaoui, A. Taamalli, A. M. Gómez-Caravaca, A. Fernández-Gutiérrez, A. Segura-Carretero, *Food Res. Int.* **2015**, *77*, 92.
[25] M. Irakli, P. Chatzopoulou, L. Ekateriniadou, *Ind. Crops Prod.* **2018**, *124*, 382.
[26] P.-J. Xie, L.-X. Huang, C.-H. Zhang, Y.-L. Zhang, *J. Funct. Foods.* **2015**, *16*, 460.
[27] R. Japón-Luján, J. M. Luque-Rodríguez, M. D. Luque De Castro, *J. Chromatogr. A* **2006**, *1108*, 76.
[28] R. Abbattista, G. Ventura, C. D. Calvano, T. R. I. Cataldi, I. Losito, *Foods* **2021**, *10*, 1236.
[29] A. Pereira, I. Ferreira, F. Marcelino, P. Valentão, P. Andrade, R. Seabra, L. Estevinho, A. Bento, J. Pereira, *Molecules* **2007**, *12*, 1153.
[30] C. Benincasa, I. Santoro, M. Nardi, A. Cassano, G. Sindona, *Molecules* **2019**, *24*, 3481.
[31] A. Romani, S. Mulas, D. Heimler, *Eur. Food Res. Technol.* **2017**, *243*, 429.
[32] C. Didaskalou, S. Buyuktiryaki, R. Kecili, C. P. Fonte, G. Szekely, *Green Chem.* **2017**, *19*, 3116.
[33] V. Voros, E. Drioli, C. Fonte, G. Szekely, *ACS Sustainable Chem. Eng.* **2019**, *7*, 18444.